PHASE MEASUREMENTS IN MICROWAVE FIELDS

PHASE MEASUREMENTS

IN

MICROWAVE FIELDS

By

LESLIE ARTHUR ALLEN READ, B.A.

A Thesis

Submitted to the Faculty of Arts and Science

in Partial Fulfulment of the Requirements

for the Degree

Master of Science

McMaster University

October 1966

MASTER OF SCIENCE (1966)
(Physics)

McMaster University
Hamilton, Ontario

TITLE: Phase Measurements in Microwave Fields

AUTHOR: Leslie Arthur Allen Read, B.A. (McMaster University)

SUPERVISOR: Professor A.B. McLay

NUMBER OF PAGES: 24, vi

SCOPE AND CONTENTS:

Two ways of measuring the relative phase in microwave fields are described in the second chapter of this thesis. The homodyne circuit is described in detail as this method was the one eventually used because of its high accuracy. Measurements were taken using a one inch dielectric rod and these were compared with theoretical predictions as calculated by previous and present laboratory workers here. Conclusions and suggestions for further work are presented in the last chapter.

ACKNOWLEDGMENTS

The author wishes to thank his research supervisor, Prof. A.B. McLay, whose careful guidance throughout the duration of this research has made it possible to present this thesis.

The author would also like to thank Mr. Hart C. Bezner, Mr. M.Z. Ali and many friends whose advice and encouragement have not gone unnoticed.

TABLE OF CONTENTS

LIST OF ILLUSTRATIONS

CHAPTER 1

INTRODUCTION

Part 1 - Light - Wave or Particle

Energy transport is as vital to life as is anything else. Yet, there are only two modes in which this can be achieved, particles and waves. This report will be concerned with a form of the latter, namely, electromagnetic waves in the microwave region.

The electromagnetic spectrum encompasses all electromagnetic waves or photons and all are identical in every respect except frequency and wavelength. The microwave region starts somewhere in the 150 cm. region of wavelength and goes down to about the 3.0 mm. wavelength. They are in effect short radio waves. This work was done in the X-band at a frequency of 9370 megacycles per second or at about 3.2 cm. wavelength.

The study of light rays is one of the oldest fields in physics. Galileo initiated the use of optical systems in scientific studies but perhaps Sir Isaac Newton made the most popular study of optics. In Newton's days the most pressing problem was whether light consisted of particles or waves. The answer or course is that electromagnetic radiation has both aspects. Interference and diffraction experiments show that it must consist of waves and yet quantum effects such as the photo-electric effect and the Compton effect can be explained only if light is assumed to consist of particle-like photons. Thus, electromagnetic radiation shows both wave and particle properties. However,

it does not show them simultaneously and not in the same experiments. This was enunciated by Niels Bohr in 1928 who stated that the wave and particle aspects of electromagnetic radiation are complementary, and has become known as the "principle of complementarity". These two aspects are complementary in that both must be known and understood but the choice of one description for an experiment definetely precludes the simultaneous application of the other description.

The phenomena of interference and diffraction of light have been known for a long time and have been described by Young and Fresnel using wave theory. Since the exploitation of the microwave region of the spectrum it has been possible to study these effects close to the subject under consideration which is completely impossible in the visible region because of the small wavelengths, typically 5000Å, involved. The size of the objects under study using microwaves can be comparable to the wavelengths used. Electromagnetic waves in the microwave region provide an excellent example of the application of Maxwell's equations when the appropriate boundary conditions are applied.

Part 2 - Scope of the Experiment

The object of this problem was to build a microwave circuit which could be used to measure relative phase within an accuracy of one or two degrees and then to measure the relative phase in some diffraction patterns. There are two methods involved in this process; the basic circuit method and the heterodyne circuit method which will be discussed in greater detail since this is the one used. This will involve theory, description of apparatus, and adjustment procedure.

The measurement of phase is as important as amplitude measurements when investigating a diffraction field or field of a radiating aperture. Some measurements using a dielectric rod, made in the direction of propogation from the rod and in a direction perpendicular to the rod are discussed.

CHAPTER 2

EXPERIMENTAL ARRANGEMENT

Part 1 - The Microwave Bridge Method

All methods of measuring phase at microwave frequencies have one common, basic characteristic and that is that the energy from the source is divided into two paths which are eventually recombined and detected. In one arm of a bridge, known as the reference arm, a calibrated phase shifter is located. In the other arm, the unknown arm, the signal whose phase is to be measured is located.

Probably the most simple method is the so-called microwave bridge method which was used by the experimenter before deciding to change to the Robertson method. This method is instructive in that the basic ideas involved in microwave phase measurements are not shrouded by complicated circuitry. The basic circuit is shown in Figure 1.

The power is divided into two branches by the directional coupler. Some of the power is fed into the unknown arm where the signal to be measured is found. This could consist of a radiating horn and a pick-up probe, which will be discussed later, feeding to the mixer. The rest of the power from the directional coupler is fed into the reference arm, through a calibrated phase shifter to the mixer, which could be a simple electric plane tee junction.

If the reference and unknown signals are of equal amplitude and completely out of phase then there will be a null in the output of the detector. Thus, the operation of the circuit is a simple matter in such

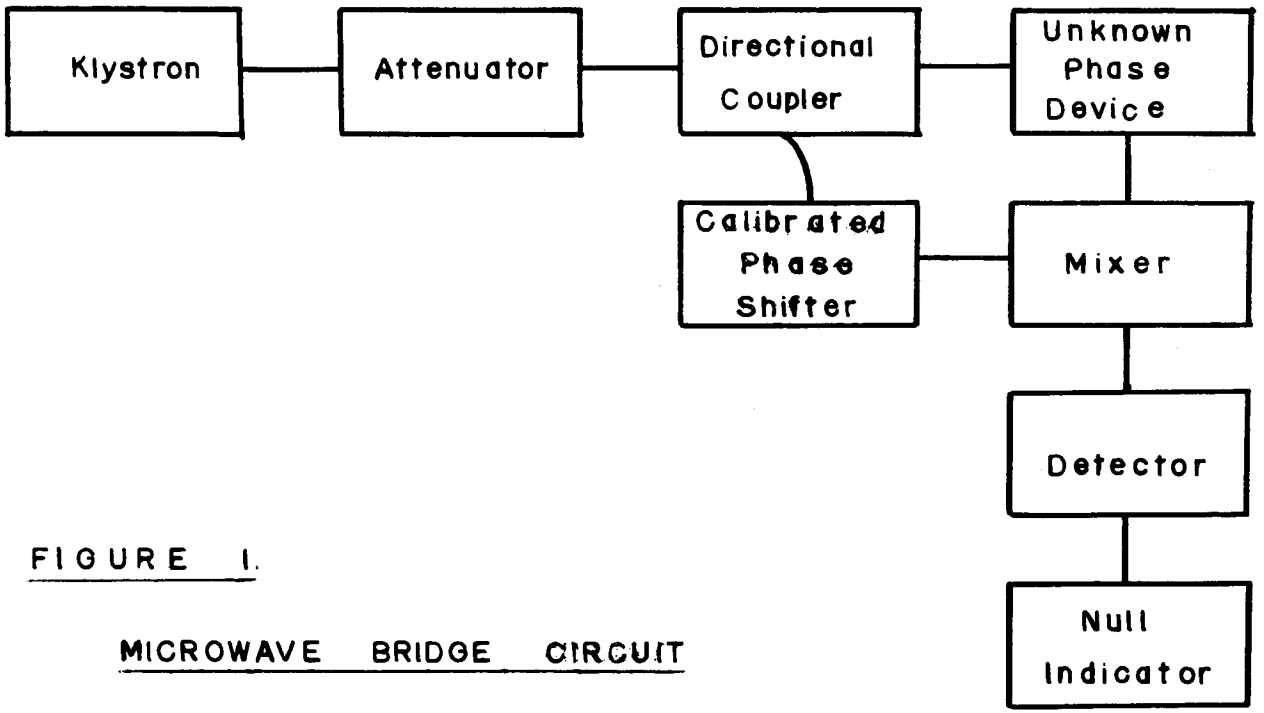

FIGURE 1.

MICROWAVE BRIDGE CIRCUIT

a case. Suppose we are investigating the phase in the radiation pattern across the aperture of an electromagnetic horn with a moveable probe. With the probe in one position the calibrated phase shifter is adjusted so as to give a null at the detector. The probe is then moved to a new position where the amplitude is assumed to be the same as before and the procedure is repeated. The difference in the two settings is the relative phase between the two probe positions.

However, this is an ideal case. We have assumed the two signals to be of equal amplitude and this is certainly not always the case. When the amplitudes are not equal then the null becomes a minimum and the accuracy of the measurement deteriorates. In fact this method becomes impractical when the ratio of the signals is about 10 db. or greater. Of course, compensating attenuators could be placed in the arms but these would have to be ones whose phase shift was very constant with attenuation. This involves too many parameters for a single measurement.

Part 2 - The Robertson "Homodyne" Method.

A method has been developed by S.D. Robertson which allows phase measurement to a relatively high degree of accuracy, even when the difference in the amplitudes of the two signals is large. (1) Essentially this involves the modulation of the signal in the unknown channel by use of a balanced modulator.

Figure 2 shows the basic circuit involved in this method and this will now be discussed in detail.

Radio frequency power is provided for the circuit from a VA-242E Reflex Klystron manufactured by Varian Associates which operates at a

FIGURE 2 THE ROBERTSON PHASE MEASURING CIRCUIT

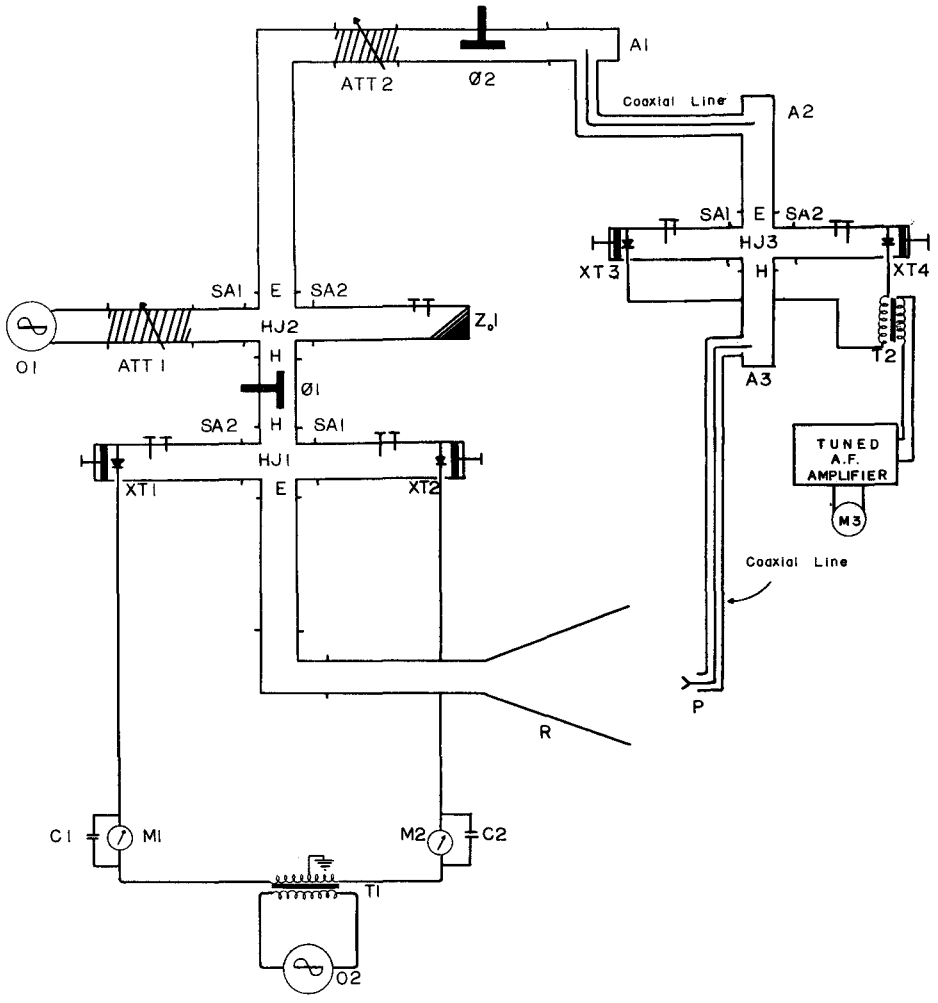

LEGEND

ATT1, ATT2 — FLAP ATTENUATORS
A1, A2, A3 — COAX TO WAVEGUIDE ADAPTORS
C1, C2 — 0.1 MFD. PAPER CONDENSERS
HJ1, HJ2, HJ3 — MICROWAVE HYBRID JUNCTIONS
M1, M2 — 0 5 MILLIAMETERS
M3 — 0 1 MILLIAMETER
O1 — 3.2 CM. SOURCE
O2 — AUDIO OSCILLATOR
P — PROBE
R — HORN TYPE RADIATING APERTURE
SA1, SA2 — HYBRID JUNCTION SIDE ARMS
T1 — HAMMOND 307 TRANSFORMER
T2 — HAMMOND 808 TRANSFORMER
XT1, XT2, XT3, XT4 — TUNNED CRYSTAL MOUNTS
$Z_0$1 — DEAD LOAD
Ø1, Ø2 — VANE TYPE PHASE SHIFTERS

frequency of 9370 megacycles per second. The klystron is capable of delivering a minimum of 500 mw. of power at a typical operating beam voltage of 500 Vdc. and a reflector voltage of -315 Vdc. The tube is cooled by a stream of forced air from any suitable fan. This also stabilizes the temperature of the klystron, thus keeping the frequency fixed. The tube is operated in the TE_{10} mode.

The 3.2 cm. radiation passes from the klystron through a variable flap attenuator which decouples the oscillator from the rest of the circuit, preventing frequency changes in the oscillator due to loading in the circuit. The power is then fed into the side arm of a hybrid junction which divides power equally between the E arm and H arm of the tee. The other side arm is terminated by a dead load which preserves the balance of the junction. Thus, the power has been divided equally into two separate channels.

Microwaves are led from the E arm into the carrier branch of the circuit consisting of an attenuator in series with the calibrated phase shifter. Generally the output of the carrier arm is much higher than that of the balanced modulator channel due to conversion loss in the modulator and loss in the microwave detection system. Thus, an attenuator is needed in the carrier branch to maintain a reasonable balance between the two signals being fed into the demodulator.

The calibrated phase shifter is a Hewlett-Packard X855A instrument and is accurate to a phase error or $\pm 2^{o}$ between any two phase settings. From the phase shifter the power is fed into a waveguide to a coaxial adapter, the latter being a type "N" coaxial connection, which feeds the demodulator.

The H arm output of the hybrid is fed through an uncalibrated phase shifter to the H arm of the balanced modulator. The purpose of this phase shifter is to adjust the phase of any sideband energy reflected back from the modulator so that it is completely quenched, thus eliminating any error here. The output of the balanced modulator, which will be discussed later, is a double sideband suppressed carrier signal which is then fed into the radiating horn.

The microwave radiation is then passed through or around the device whose relative phase pattern is to be measured and picked up at the point of measurement by an r.f. dipole probe. The power from the probe is fed via coaxial cable and then waveguide to the demodulator. All coaxial cables used in this circuit are RG - 8/U cables and as little overall length as possible is used because of the large microwave loss in them. In order to keep the length of coaxial cable used to a minimum, waveguide was used from the bottom of the probe holder to the H arm of the hybrid tee in the demodulator, a distance of about 250 cm. If coaxial cable had been used instead of waveguide here the signal fed into the demodulator would have been too small to be of any use.

The output of the demodulator is fed to a Hammond 808 transformer as shown. The signal is then displayed on a Type 503 Tectronix Oscilloscope which amplifies the signal and displays it on the Cathode Ray Tube.

Part 3 - The Balanced Modulator

The microwave balanced modulator is the most important part of the circuit. It is shown in Figure 4. The main purpose of this

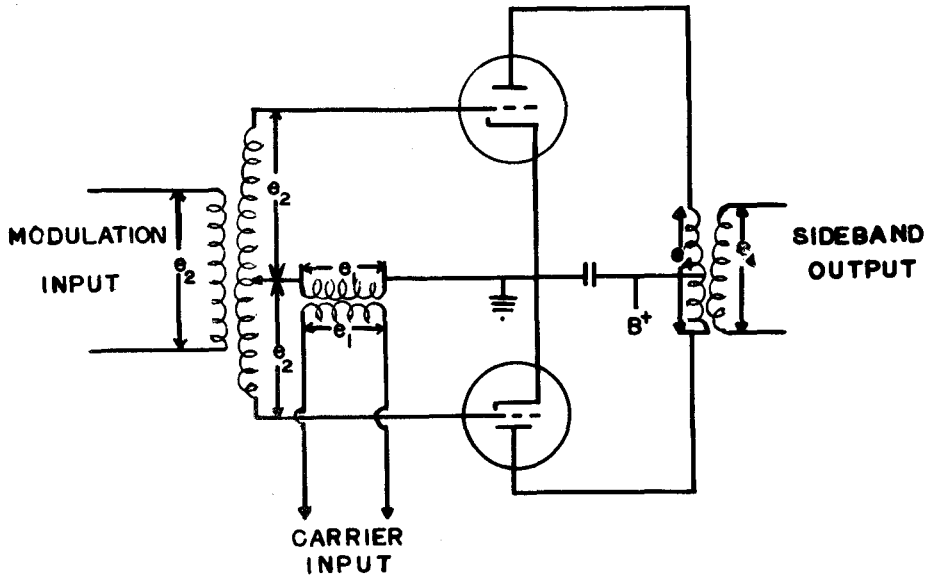

FIGURE 3. VACUUM TUBE BALANCED MODULATOR

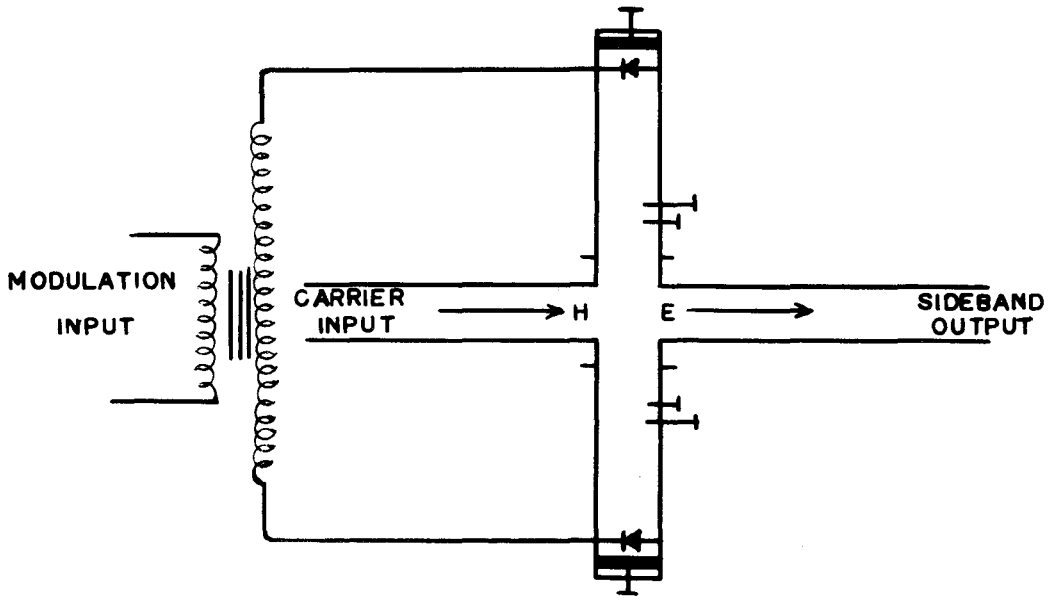

FIGURE 4. MICROWAVE BALANCED MODULATOR

modulator is to convert the carrier energy into suppressed carrier double sideband energy which is then propogated into the unknown branch of the microwave bridge. The operation of this modulator is best understood by analogy with the vacuum tube balanced modulator shown in Figure 3. The various voltages are adjusted so that the tubes are operating over that portion of the characteristics with considerable curvature. Let the dynamic characteristics of the tube be such that they can be represented by a power series.

$$i_p = a_1 e_g + a_2 e_g^2 \qquad \text{TUBE 1}$$

$$i_p' = a_1 e_g' + a_2 e_g'^2 \qquad \text{TUBE 2}$$

Thus, it is possible to write

$$e_g = e_1 + e_2$$

$$e_g' = e_1 - e_2$$

$$\therefore\ i_p = a_1 (e_1 + e_2) + a_2 (e_1 + e_2)^2$$

$$i_p' = a_1 (e_1 - e_2) + a_2 (e_1 - e_2)^2$$

Because the circuit is a difference amplifier the voltage is proportional to $(i_p - i_p')$, i.e., $e_4 = A(i_p - i_p')$

$$\therefore\ e_4 = D[a_1 a_2 + 2 a_2 e_1 e_2]$$

Let $e_1 = E_c \cos \omega_c t$, $e_2 = E_m \cos \omega_m t$

$$\therefore\ e_1 e_2 = \frac{1}{2} E_m E_c [\cos(\omega_c - \omega_m)t + \cos(\omega_c + \omega_m)t]$$

Thus, since the impedance in the output circuit is negligible to the original modulating frequency, the balanced modulator output is a double sideband suppressed carrier wave. (2)

In the waveguide circuit, Figure 4, the components are a hybrid junction whose sidearms are each terminated by a tunable crystal mount. The carrier wave is fed into the H arm and the sideband output is taken from the E arm. The two cyrstals, IN23C diode detectors, are driven

180° out of phase by a Heathkit Audio Generator operating at about 1 kilocycles per second. The audio power is passed through a Hammond 307, balanced line to line transformer. The modulating circuit also supplies a d.c. load to the crystals. As a result a d.c. bias, due to rectified crystal current, is developed in each crystal circuit on the application of either r.f. energy fed into the waveguide circuit or of audio modulating energy directly across the crystal terminals. (2) The rectified current flowing in each crystal is indicated by the d.c. milliammeter as shown in the circuit diagram of Figure 2. The capacitors prevent audio voltage drop from occurring across the meters.

The magnitude and phase of the r.f. energy reflected by each crystal or of its impedance in the mount is a function of the d.c. bias applied to the crystal, operating of course in the desired region of the crystal characteristics. Thus, if the input level is constant the impedance or load offered by each side arm is a sinusoidal function whose frequency is the modulating audio frequency being applied to the crystals and since the two arms are operated 180° out of phase the output of the modulator is a double sideband suppressed carrier wave whose two components differ from the original signal frequency. If f_c is the carrier input, 9370 mc/sec in our case and f_a the audio input, the two output components are $(f_c + f_a)$ and $(f_c - f_a)$, as demonstrated earlier in the case of the vacuum tube circuit.

Part 4 - The Detecting Device

When the path difference between the two branches is such that at the detector the carrier phase in the reference arm is 90° ahead or

behind the carrier phase in the amplitude modulated wave, the output of the detector contains no component of amplitude modulation at the original modulation frequency. Thus, if the amplifier used is tuned to the audio modulation frequency the detector will indicate a null whenever the homodyne carrier is brought in quadrature with the signal for two different phases 180° apart. This sharp null occurs over a large range of relative amplitudes of the carrier and sideband signals.

This action can be explained in two ways. It can be looked at by a vectorial method or shown mathematically. Consider first the vectorial demonstration as shown in Figure 5.

In Figure 5 (a) the carrier is in phase with the two sidebands. The carrier is the reference vector, C, at fixed phase. The two sidebands are then equal amplitude vectors rotating with equal and opposite angular velocities, W_a. The figure shows the resultant at five different points in the modulation frequency cycle. The resultant, R, goes through an amplitude cycle equal to the cycle of the modulating frequency without any variation of phase. Here the important thing is that the amplitude variation of the resultant is the same as that of the modulating signal.

Consider now the resultant of Figure 5 (b) where the carrier has been rotated through 90° from the previous case. The resultant is shown at the same five points in the modulating frequency cycle as in (a). Now, however, there is a pronounced phase modulation of the resultant vector and still some amplitude modulation. But, the complete cycle of the amplitude variation of the resultant now occurs in exactly one half the period of the modulating frequency cycle. That is, the amplitude modulation in the quadrature case has a period equal to that of the

FIGURE 5 VECTOR DEMONSTRATION OF OPERATION OF "HOMODYNE" DETECTION PRINCIPLE.

(a) Carrier in phase with sidebands

(b) Carrier in quadrature with sidebands (Null Condition)

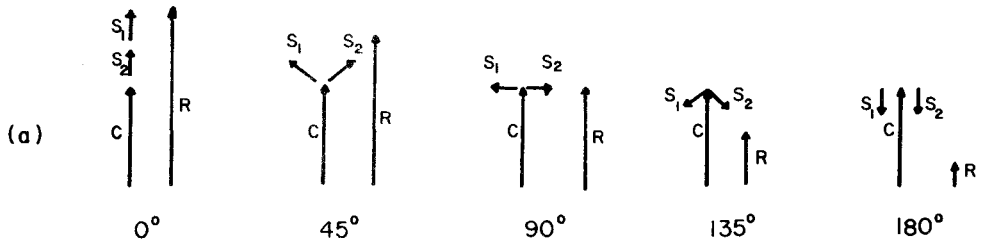

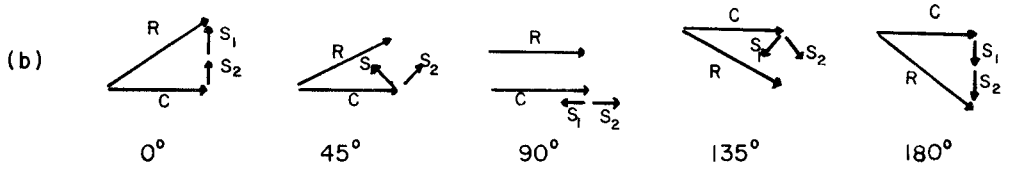

LEGEND

C – Carrier

S_1 – Upper sideband

S_2 – Lower sideband

R – Resultant

second harmonic of the modulating signal. (2)

Any point between these two extremes can be resolved into components of both. Looking at this phenomena mathematically, the expression for an amplitude modulated wave, modulation factor m, is written as

$$\psi = A(1 + m\cos\omega_a t)\cos\omega_c t \quad , \qquad \omega_i = 2\pi f_i$$

$$\psi = A\cos\omega_c t + Am\cos\omega_a t\cos\omega_c t$$

$$\psi = A\cos\omega_c t + \frac{Am}{2}\left[\cos(\omega_c+\omega_a)t + \cos(\omega_c-\omega_a)t\right] \quad (1)$$

Let the two sidebands be shifted in phase by 90° with respect to the carrier. Thus equation (1) becomes

$$\psi = A\cos\omega_c t + \frac{Am}{2}\left[\cos\left[(\omega_c+\omega_a)t+\frac{\pi}{2}\right] + \cos\left[(\omega_c-\omega_a)t+\frac{\pi}{2}\right]\right]$$

$$\psi = A\left[\cos\omega_c t - \frac{m}{2}\left\{\sin(\omega_c+\omega_a)t + \sin(\omega_c-\omega_a)t\right\}\right]$$

$$\psi = A\left[\cos\omega_c t - m\sin\omega_c t\cos\omega_a t\right]$$

$$\psi = \sqrt{1 + m^2\cos^2\omega_a t}\;\cos\left(\omega_c t + \tan^{-1} m\cos\omega_a t\right)$$

If $m \ll 1$ the square root can be expanded by the Binomial Theorem. Neglecting powers higher than the second the wave function becomes

$$\psi = A\left\{1 + \frac{m^2}{2}\cos^2\omega_a t\right\}\cos(\omega_c t + \tan^{-1} m\cos\omega_a t)$$

$$\psi = A\left\{1 + \frac{m^2}{2}\left(\frac{1}{2} + \frac{1}{2}\cos 2\omega_a t\right)\right\}\cos(\omega_c t + \tan^{-1} m\cos\omega_a t)$$

$$\psi = A\left\{\left(1 + \frac{m^2}{4}\right)\left(1 + \frac{m^2}{m^2+4}\cos 2\omega_a t\right)\right\}\cos(\omega_c t + \tan^{-1} m\cos\omega_a t)$$

Thus, the amplitude modulation is at twice the modulating frequency.

Part 5 - The Balanced Demodulator

The balanced demodulator is similar to the balanced modulator

in design and importance. The side arms of a hybrid tee are terminated with tunable crystal mounts and fitted with two matched IN23C crystals. The signal from the unknown branch is fed into the H arm and the signal from the reference branch is fed into the E arm of the tee. The purpose of the hybrid junction is to prevent errors due to interbranch coupling by isolating the carrier and sideband branches. This part of the circuit works in reverse to the balanced modulator. Here the voltage generated across the two diodes, 180° out of phase, due to the input, is fed through a balanced transformer, a Hammond 808. The output from the transformer is displayed on the oscilloscope. If necessary the audio signal will have to be amplified before being fed to the oscilloscope or some other null-indicating device.

Part 6 - The R.F. Probe and Track Assembly

The probe used for measurements was a "choke" or "quarterwave can" dipole. (3) (4) This is shown in detail in Figure 6.

In effect this is a shorted quarter-wave-length series stub which presents an infinite impedance to currents attempting to flow back in the cable to the dipole. Thus, the dipole should not reradiate microwaves. The balanced sleeve was a piece of copper tubing large enough to fit snugly around the outside conductor of the coaxial cable and was 0.8 cm. long. The probe and cable were held in a curved glass rod as shown in Figure 7. The rod was fixed in a probe carriage to a track. The carriage could be moved linearly along the track by means of a worm gear, 175 cm. in length, which is driven by a Hoover, 1/8 H.P., A.C. motor coupled to a 100 : 1 Boston Gear Reducer. With this arrange-

FIGURE 6 R.F. "CHOKE" DIPOLE PROBE

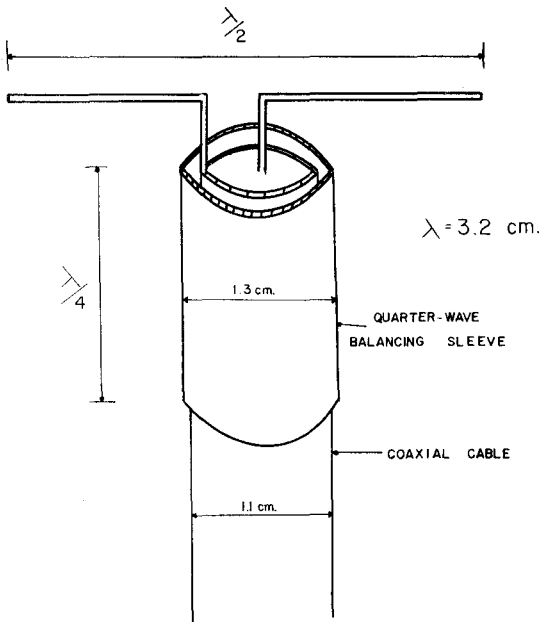

FIGURE 7 PROBE HOLDER

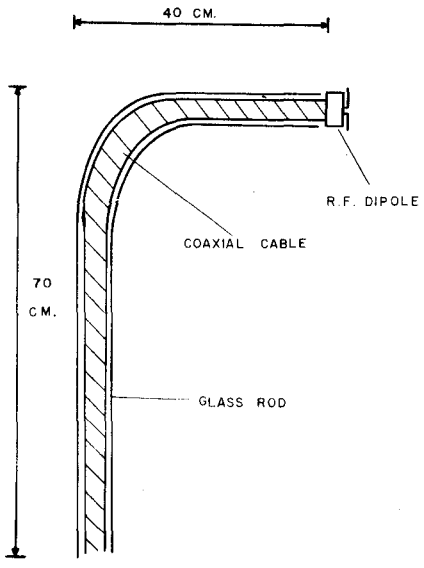

ment the probe can be driven along at a rate of 0.68± 0.001 mm./second. The whole assembly is shown in Figure 8.

Part 7 - Circuit Adjustment Procedure

There are certain waveguide components in the circuit which must be adjusted to certain specifications before they can be used successfully. The dead load Z_o1, see Figure 2, must be adjusted to a standing wave ratio of unity in order to absorb all incident power without reflection. The adjustment is made by putting an oscillator, attenuator, and standing wave detector, in series with the dead load and adjusting the two small screws tapped into the guide wall until the desired ratio is achieved.

The most critical components to be adjusted are the tuned crystal mounts. For each pair of mounts XT1, XT2 and XT3, XT4 the crystals chosen must be ones whose d.c. front and back resistances are balanced within 10% and the ratio of front to back resistance is at least 20 to 1. Once this has been accomplished then each mount should be adjusted to unity standing wave ratio as outlined above.

When the circuit is completed, the frequency is stabilized by allowing the equipment to warm up for about an hour. The two meters M1 and M2, see Figure 2, should read close to the same value, having matched the crystals, and after the amplifier is tuned the meter M3 should have a reading except for a sharp null at some position of the calibrated phase shifter. If no amplifier is used but simply an oscilloscope as in the actual case here then the null will be seen as complete absence of a signal at the modulating frequency. The signal seen on the

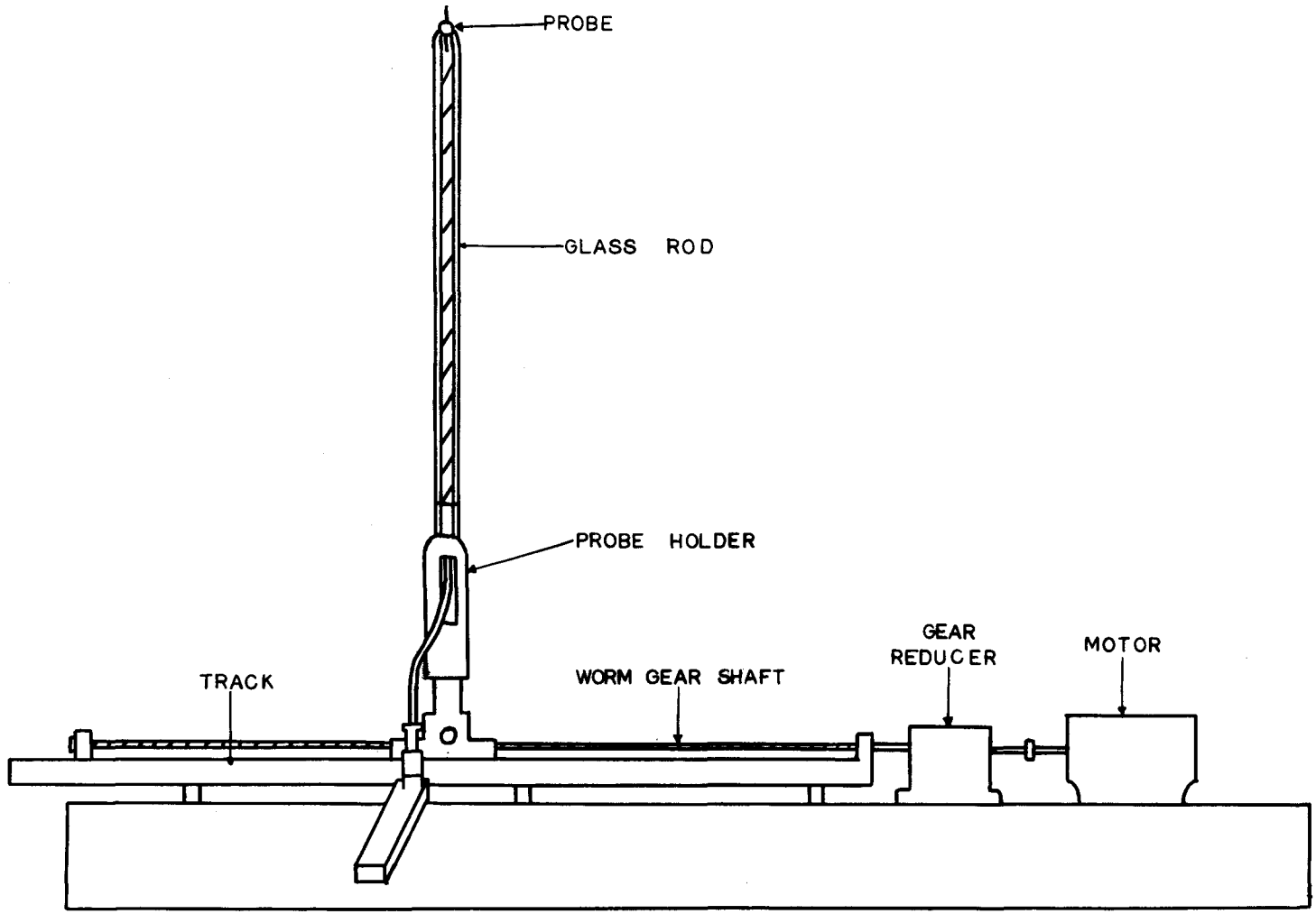

FIGURE 8. TRACK AND PROBE ASSEMBLY

oscilloscope will be that of the second harmonic of the modulating frequency as described in Part 4 of this chapter.

Usually the carrier is not completely suppressed in the output of the balanced modulator. Since the residual carrier will be added to the homodyne carrier in the detector, and since the null adjustment will be reached when the resultant carrier is in quadrature with the sidebands, it is desirable that the residual carrier be low in level compared with the homodyne carrier. (1) The error due to the residual carrier in the sideband arm is shown in Figure 9.

The figure would be similar for the error due to residual sideband in the carrier arm. This reason for error is eliminated by adjustment of the phase shifter $\varphi 1$ in Figure 2. This is achieved by first disconnecting the sideband input to the detector by removing the connection at A2. Then $\varphi 1$ is adjusted to a null at the output.

Thus, the two main adjustments are to have no residual carrier in the sideband branch by modulator balance, and to have no residual sideband in the carrier branch by the adjustment of $\varphi 1$. The two branches must be completely isolated. If these two conditions are met then there will be two nulls, exactly 180° apart; when the reference carrier is in exact quadrature, ahead or behind the sideband energy. If the two nulls are not 180° apart then either or both adjustment procedures must be repeated.

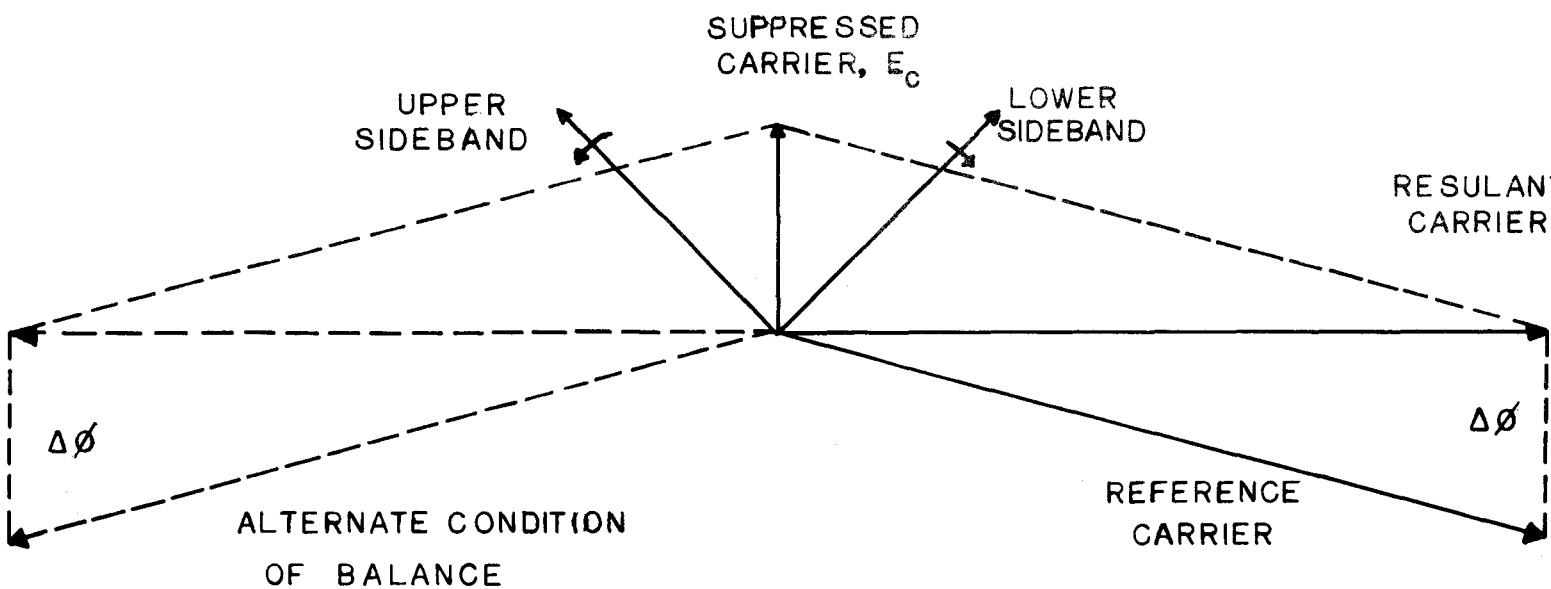

FIGURE 9. ERROR DUE TO RESIDUAL CARRIER IN SIDEBAND ARM

CHAPTER 3

DIFFRACTION BY A CYLINDRICAL DIELECTRIC ROD

Part 1 - Diffraction by a Dielectric Rod

Equations for the diffraction by a dielectric rod have been given by Froese and Wait. (5) The geometry for the problem is shown in Figure 10.

The point S is the geometrical apex of the radiating horn, O is the center of the rod and the rest of the diagram is self-explanatory. There are two special cases, namely when the polarization of the incident electric vector is parallel and when it is perpendicular to the axis of the rod. Since the experimental results deal with the former case, only this will be considered here. The field E_z at P normalized to the incident field E_o at P, if x_o is much larger than "a" and "x", is

$$\frac{E_z}{E_o} = e^{i\varphi_o} + \sum_{m=0}^{\infty} C_m i^m H_m^{(1)}(k\rho) A_m \cos(m\Phi) \qquad (1)$$

where $\varphi_o = k\left(\sqrt{(x+x_o)^2 + y^2} - x_o\right)$

$k = \frac{2\pi}{\lambda}$ λ = free space wavelength

$C_o = 1$; $C_m = 2 \; (m \neq 0)$

$\rho = (x^2 + y^2)^{1/2}$ $\Phi = \tan^{-1}(y/x)$

and

$$A_m = - \frac{n J_m(ka) J_m'(Nka) - J_m'(ka) J_m(nka)}{n H_m^{(1)}(ka) J_m'(Nka) - H_m'^{(1)}(ka) J_m(Nka)}$$

where $n = (\mu_o \epsilon_1 / \mu_1 \epsilon_o)^{1/2}$, $N = (\epsilon_1/\epsilon_o)^{1/2} (\mu_1/\mu_o)^{1/2}$

Here the dielectric constant and permeability of the rod are ϵ_1 and μ_1 respectively and ϵ_o and μ_o are the corresponding quantities for the medium of propogation. The permeabilities have been set equal to

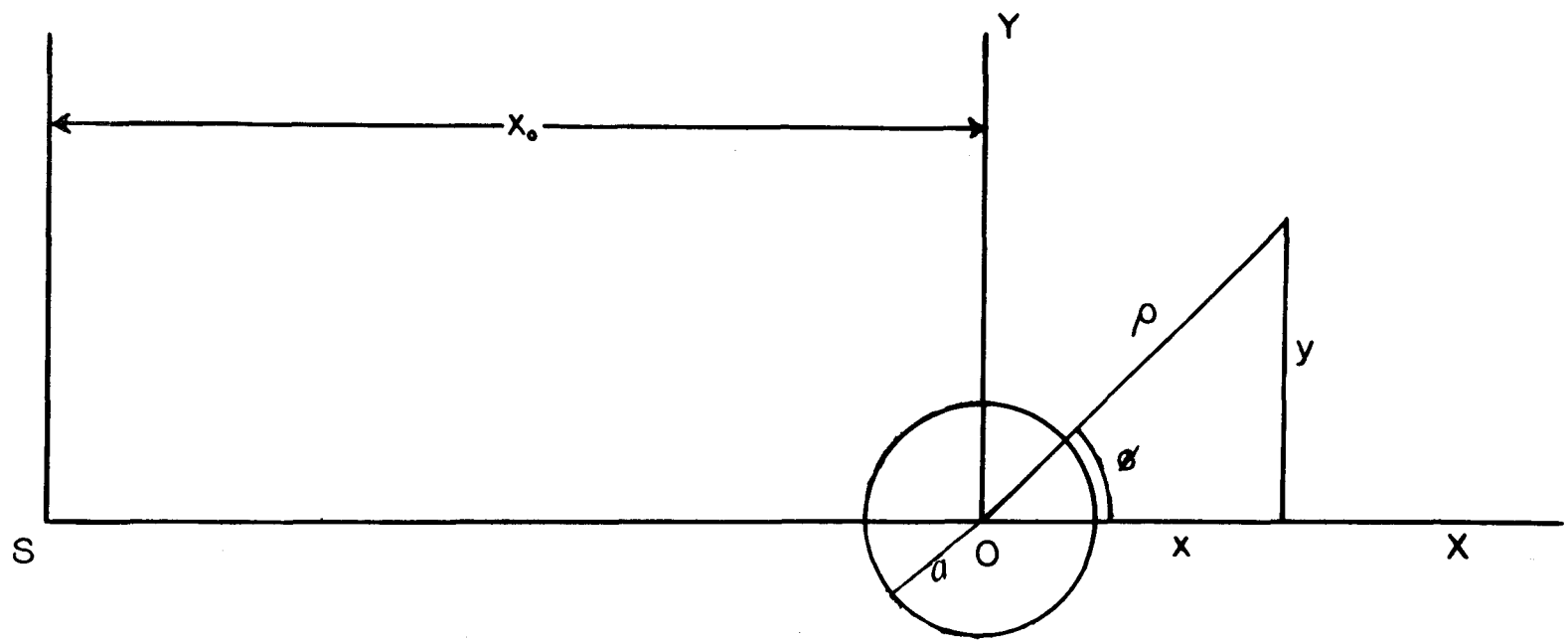

FIGURE 10. GEOMETRY FOR DIELECTRIC CYLINDER OF RADIUS a.

unity for calculations in this thesis. J_m and $H_m^{(1)}$ are the usual notation for the Bessel and Hankel functions (see Ref. 5).

Equation (1) is derived from the assumption that the incident field is a cylindrical one. That is, the radiation from the horn has a cylindrical wavefront instead of a plane wave front. We shall examine the two terms on the right-hand side of Equation (1). The first term is due to the incident field and the second term, the summation, is due to the scattered field. If the incident wave had been plane then the first term would have been e^{ikx} but since the incident wavefront is a cylindrical one a correction must be made to this term, and it can be seen that $e^{i\phi_o}$ is the correct expression for a cylindrically outgoing wavefront. The second term we are dealing with here is the summation term and is that part of the diffracted wave due to the scattering from the rod. In order to determine the correct form of the scattered wave, the incident field at the cylindrical body is all that must be known. If x_o is large enough, then over the limited region of the cylinder it may be assumed that the incident wave is plane. This being the case, this term has been derived using the assumption that the wavefront incident on the rod is a plane one.

A value of 250 cm. was chosen for x_o and so the theoretical calculations where made for this distance.

Part 2 - Experimental Procedure

The procedure will be outlined for the $\Phi = 90^o$ case, i.e., when the probe is moved in the y direction. When the probe is moved in the x direction the procedure is similar and need not be repeated.

Several adjustments must be made before placing the dielectric rod is the field. The distance from horn to probe must be made equal to 250 cm. first. It is assumed that the microwave circuit has been adjusted as described earlier. At this point the power output of the modulator should be large enough so that the output of the demodulator is such that the phase adjustment can be easily made within a $\pm 5^{o}$ range. If more power is needed the beam voltage of the klystron will have to be increased and the reflector voltage readjusted so that the klystron is operating in the center of the TE_{10} mode.

The most critical adjustment at this time is the positioning of the track. The geometrical center of the pattern must coincide with the experimental center. The simplest way to do this is to make measurements of the phase of the radiation pattern of the horn at x_o = 250 cm. as shown in Figure 11 and to adjust the position of the track until the two centers coincide as shown.

A dielectric rod of lucite, with 1.233 cm. radius, was placed at the center of the pattern and the probe was moved along in the y direction. The measurements were taken at equal intervals using an electronic phototimer.

Part 3 - Presentation of Results

Both theoretical calculations and experimental measurements have been made for the diffraction by the rod for x_o = 250 cm. On the following series of graphs, Figures 12, 13, and 14, both will appear for the sake of comparison.

Consider first Figure 12 which shows the phase variation for

FIGURE 11.

Phase Measurement across Horn Aperture

$x_o = 250$ cm.

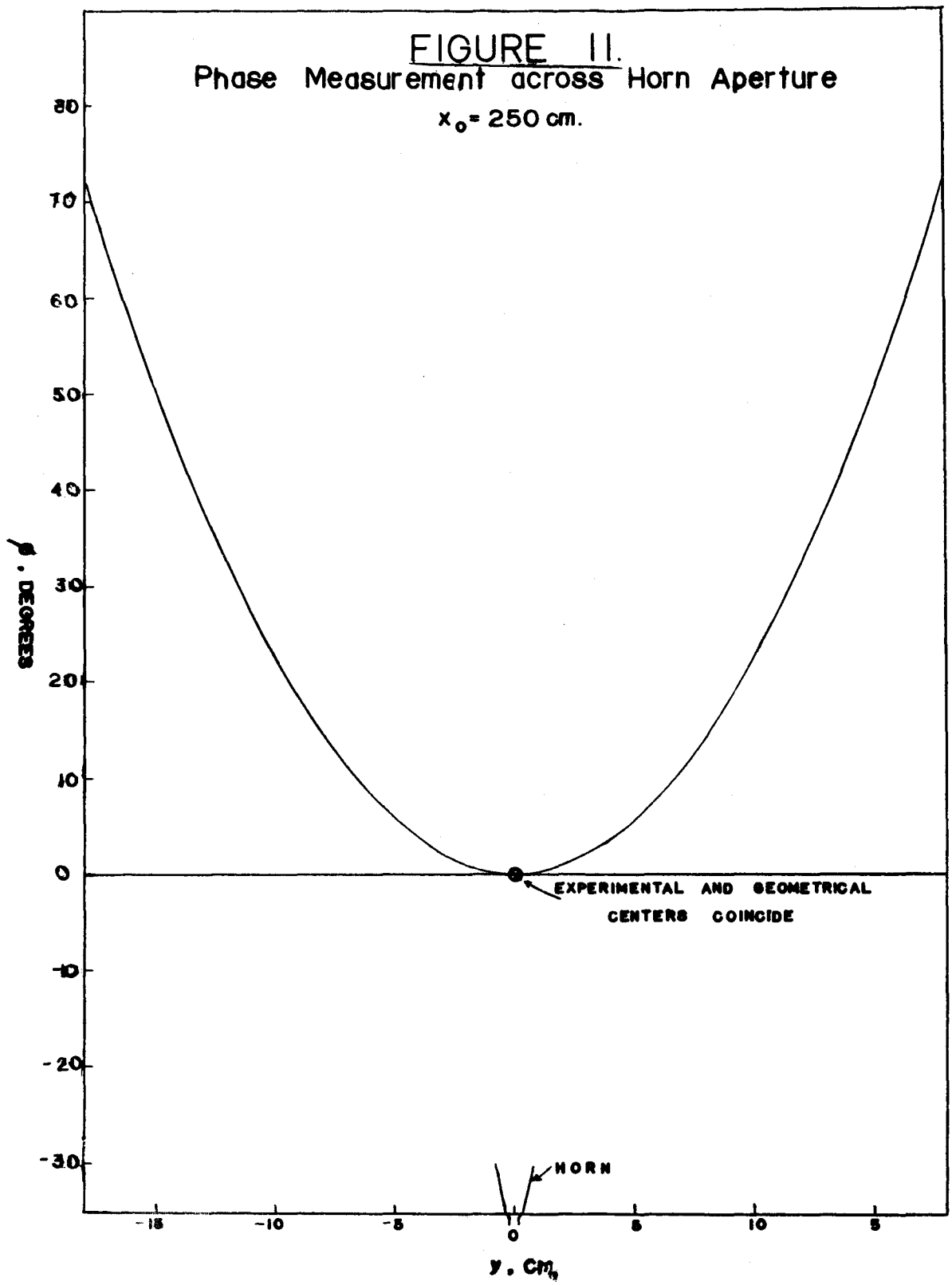

diffraction by the dielectric rod for $\Phi = 90^{o}$, i.e., along the y-axis away from the rod for x = o. The solid curve represents the theoretical calculations of the dependence of $(\phi - \phi_o)$ on the distance y. The experimental points for this situation are the dots with the circles surrounding them. The distance measured along the y-axis is given in centimeters from the center of the rod. No points could be recorded closer than 2.0 cm. from the center of the rod because of the finite widths of the probe and the rod.

As is seen in this figure the theoretical calculations have been made only as far as 8.0 cm. in the y direction and the experimental points have been taken up to y = 14.0 cm. The points lie quite close to the theoretical values and follow the same sinusoidal variation as the calculations. Thus, the readings between y = 8.0 cm. and y = 14.0 cm. should also be quite close to the values predicted by theory. The points are equispaced because the movement of the probe was controlled by an electronic phototimer which was set at 3 sec. and not altered throughout the course of a run. This means that the distance between the point-to-point measurements was the same through one complete run and since the phototimer was used it is felt that the error in the spacing of the points along the y-axis is negligible.

The reason for plotting $(\phi - \phi_o)$ versus y instead of simply ϕ is an important consideration at this point. The expression $(\phi - \phi_o)$ simply means the difference in phase between the situation when the dielectric rod is in the incident microwave field and the situation when the rod is not in the incident microwave field. In other words, it gives the change of phase resulting from the diffracting effects

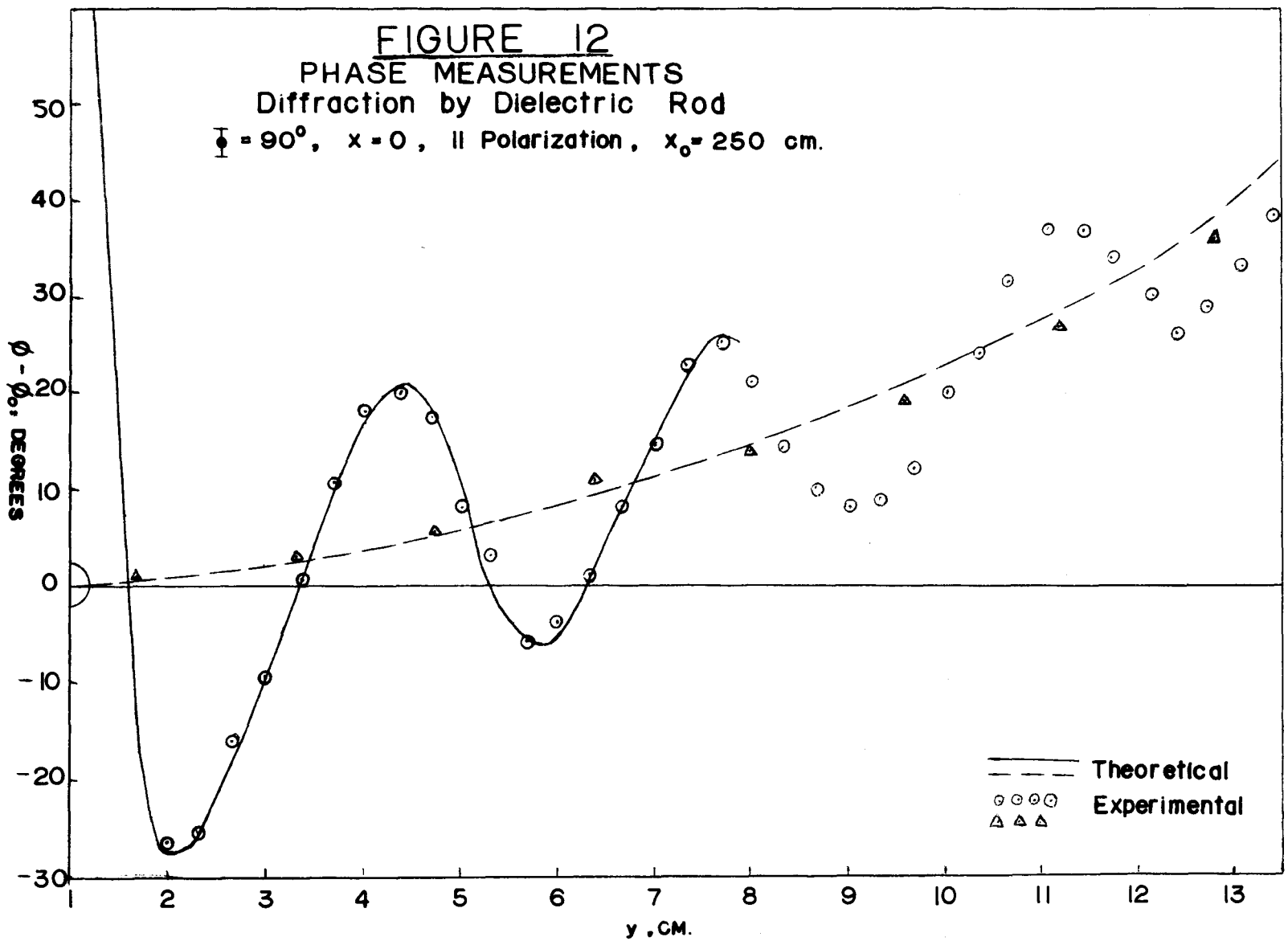
FIGURE 12
PHASE MEASUREMENTS
Diffraction by Dielectric Rod
= 90°, x = 0, ll Polarization, x_0 = 250 cm.
$\phi - \phi_0$, DEGREES
y, CM.
Theoretical
Experimental

produced by a dielectric rod in a microwave field.

The dotted line in this figure is a theoretical calculation of incident field for this case. Of course, here just ϕ is plotted against y because the rod is not in the field. The experimental points for this curve are the dots with the triangles around them. As can be seen the scattered field does vary about the incident field quite nicely with the peaks and troughs getting smaller further away from the rod.

Figure 13 shows the phase variation for diffraction by the dielectric rod for $\Phi = 0^{o}$, i.e., along the x-axis away from the rod for $y = 0$. In this figure $(\phi - \phi_{o})$ is plotted versus the y distance for the same reason as for Figure 12. As before the theoretical curve is the solid line and the experimental values are the encircled dots.

Figure 14 displays the same results as Figure 13 but in a slightly different way. Here, just ϕ is plotted against x. The reason for this is to show the accuracy of the circuit in measuring the phase variation over a 450^{o} range. As can be seen the experimental results lie very close to the theoretical curve.

Thus, the phase variation for these two simple cases of diffraction by a dielectric rod is quite different upon comparison of Figures 12 and 13 and the heterodyne circuit appears capable of good measurements for both situations.

Part 4 - Accuracy of Results

Comparing the experimental values with predicted values on the preceding figures, it can be seen that the accuracy of the homodyne method of measuring phase is quite high in this experiment. In fact,

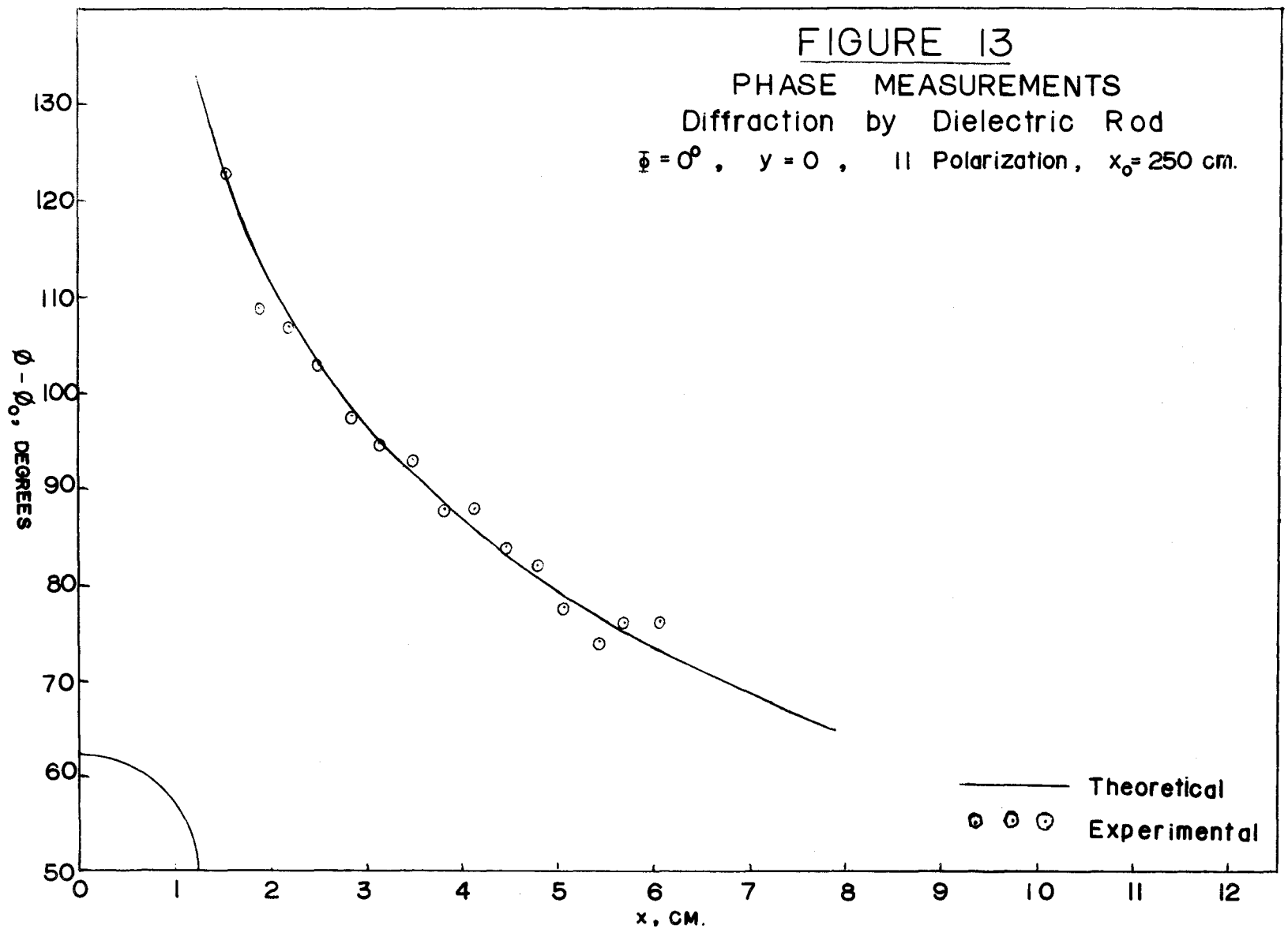
FIGURE 13
PHASE MEASUREMENTS
Diffraction by Dielectric Rod
Φ = 0° , y = 0 , ⊥ Polarization , x0 = 250 cm.
Ø - Ø0, DEGREES
130
120
110
100
90
80
70
60
50
0
1
2
3
4
5
6
7
8
9
10
11
12
x, CM.
Theoretical
Experimental

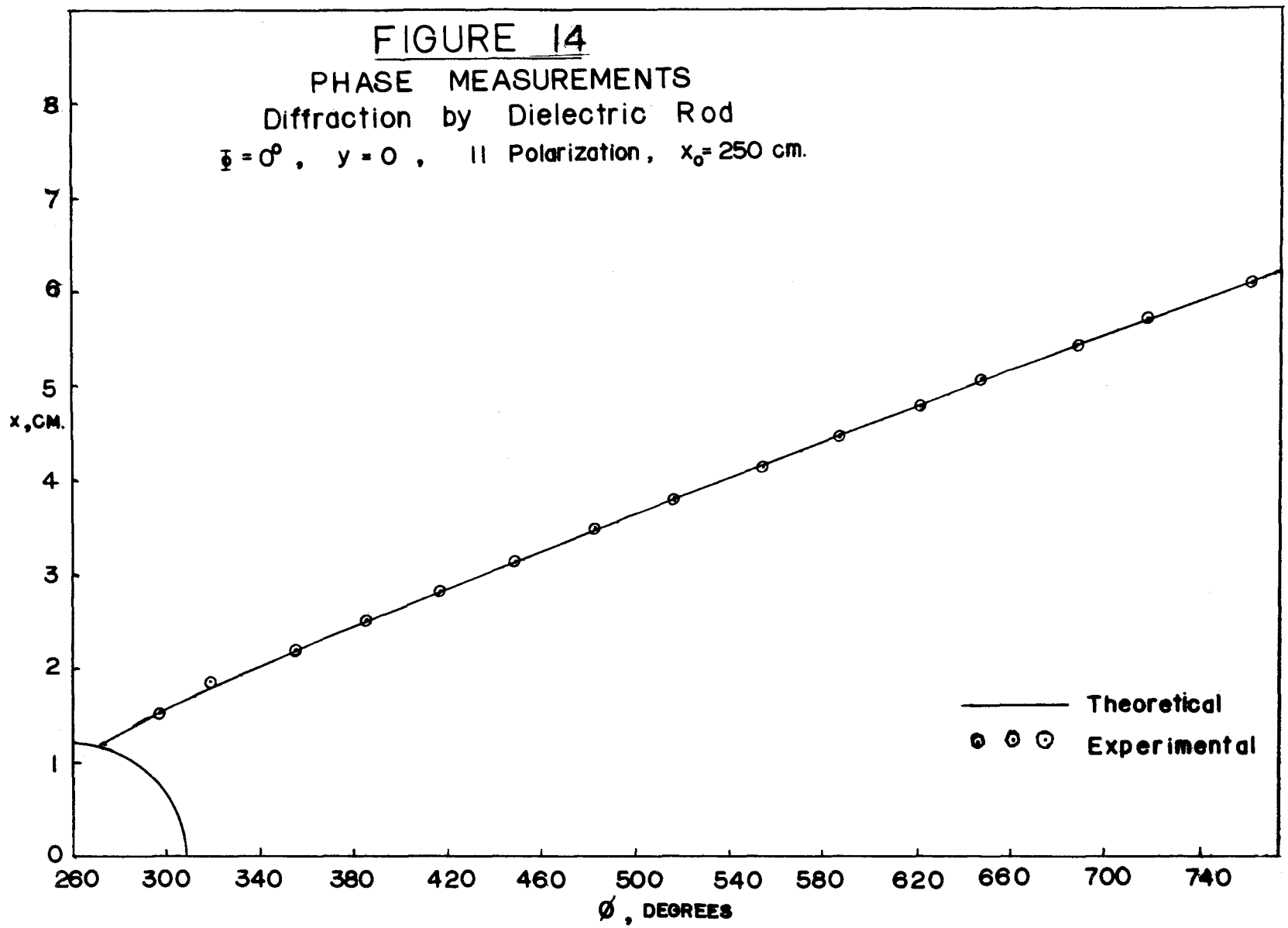
FIGURE 14
PHASE MEASUREMENTS
Diffraction by Dielectric Rod
Φ = 0° , y = 0 , ⊥ Polarization , x0 = 250 cm.
x, CM.
0
1
2
3
4
5
6
7
8
260
300
340
380
420
460
500
540
580
620
660
700
740
Ø , DEGREES
Theoretical
Experimental

the results here are as good as or better than any seen in published results in this field. (6) (7) There are, however, several important sources of error in the experiment.

The specifications on the Hewlett Packard Phase Shifter X855A give a maximum error of $\pm$ 2° between any two settings of the phase shifter. This error cannot be made smaller unless a phase shifter is made personally by the experimenter, which would take much time and effort, not to mention the great precision which would have to be prevelant in the manufacturing process.

As mentioned in Chapter 2, Part 7, errors will arise due to residual sideband in the carrier arm and residual carrier in the sideband arm. Adjustment procedures were given earlier for reduction of this error but it is felt that this error cannot be neglected completely.

The finite size of the probe may also create some error. Its mere presence in the field does disturb the true field somewhat but to what extent this happens is not known to the experimenter. The other major source of error is in the null detection system. As described in Chapter 2 the output of the 808 Transformer was fed directly into the oscilloscope. Because the input signal was rather small the vertical gain control on the scope had to be turned quite high, thus losing some stability of the trace. In most cases the null could be established to within plus or minus one or two degrees with this method. However, using a tuned audio amplifier instead of an oscilloscope may prove to be more accurate.

In lieu of all these possible sources of error it is felt that the point-to-point measurements presented in this chapter have an

accuracy of $\pm$ 3 to $\pm$ 4 degrees of phase. However, with care in technique and equipment this value may be reduced.

CHAPTER 4

CONCLUSIONS AND PROPOSALS FOR FURTHER WORK

The most accurate system known at present for measuring phase in microwave fields is the so-called "Robertson Homodyne" method used here. The investigations here involved the construction of apparatus and the testing of it for accuracy by comparison of experimental and theoretical results. For the purposes of testing the equipment the phase of a diffracted wave using a dielectric rod was measured. Measurements were made in two directions in the plane of the rod, perpendicular to the direction of propagation, and in the direction of propagation, using parallel polarized microwaves, i.e., the electric vector was parallel to the axis of the rod. These measurements were seen to agree with those predicted by theory allowing for an accuracy of $\pm$ 3 or $\pm$ 4 degrees of phase.

It should be emphasized that this circuit can be used for any type of diffraction measurements involving microwaves which could include investigations with such objects as prisms or lenses presently being used by Hart Bezner in this microwave laboratory.

Some improvements to the circuit have been mentioned in Chapter 3, Part 4. One further refinement which would vastly improve the apparatus would be to make the circuit automatic. This would involve feeding the output of the tuned amplifier to a reversible motor which would drive the phase shifter to its null point. The phase shifter could in turn drive a pen recorder. Instead of point-to-point measure-

ments this would give a continuous record of the phase in a diffraction pattern as the probe was moved across the microwave field.

BIBLIOGRAPHY

(1) Robertson, S. D., A Method of Measuring Phase at Microwave Frequencies, Bell Syst. Tech. Journal, 28, 99, 1949

(2) Ornstein, W., Phase Measurements in Microwave Fields, M. Sc. Thesis, McGill University, August, 1949

(3) Barlow, H. M., and Cullen, A. L., Microwave Measurements, Constable and Company, London, 1950

(4) King, D. D., Measurements at Centimeter Wavelengths, D. Van Nostrand, New York, 1952

(5) Froese, C. and Wait, J. R., Calculated Diffraction Patterns of Dielectric Rods at Centimetric Wavelengths, Can. J. Phys., 32, 775, 1954

(6) Wiles, S. T., Diffraction of Microwaves, M. Sc. Thesis, McMaster University, October, 1952

(7) Kodis, R. D., J. Appl. Phys., 23, 249, 1952